Journal of Applied Geodesy 2 (2008), 233–238 © de Gruyter 2008. DOI 10.1515/JAG.2008.026
First published in:

Reference point determination with a new mathematical model at the 20 m VLBI radio telescope in Wettzell

Michael Lösler

Abstract. A new mathematical model to estimate the International VLBI Service (IVS) reference point and additional parameters of a Very Long Baseline Interferometry (VLBI) radio telescope was developed by Lösler and Hennes (2008). To verify this analysis procedure a reference point determination was carried out on the 20 m radio telescope at the "Fundamentalstation Wettzell" (Germany) from April to May 2008. This paper describes the terrestrial local survey, the analysis methodology and the results obtained, in particular the accuracy of the determination of the IVS reference point.

Keywords. Local tie, VLBI, reference point determination, mathematical model, geodetic surveys.

1. Instruction

The Fundamentalstation Wettzell (Germany), operated by the Bundesamt für Kartographie und Geodäsie (BKG), is a co-located station. This means it hosts instrumentation from different space geodetic techniques such as Very Long Baseline Interferometry (VLBI), Global Navigation Satellite System (GNSS) and Satellite/Lunar Laser Ranging (SLR/LLR). To combine these different space observing systems, the reference point of each technique and the 3D relationship is needed in a common reference frame, which can be transformed into a global one. The reference point of the 20 m VLBI radio telescope was measured in relation to the local site network from April to May 2008. This point is defined as the intersection between the azimuth-axis and elevation-axis of the telescope. If these axes do not intersect, the reference point is the projection of the elevation-axis onto the azimuth-axis which has the shortest/minimum distance to the elevation-axis. The advantage of this definition is that the geometrical reference point is invariant in every telescope position, but the drawback is that it is also inaccessible for direct survey measurements. Hence, it is only possible to estimate the reference point indirectly by observing the trajectory of some targets on the telescope structure. For this a new algorithm was developed (Lösler and Hennes 2008) and has been verified with observation data from the local survey in Wettzell (Germany).

The main difference between the new mathematical model and the established 3D circle-fitting methods (e.g. Eschelbach and Haas 2003, or Dawson et al. 2006) is that, in principle, no terrestrial observations of predefined telescope positions are needed. Therefore, a measurement during telescope motion is possible, and hence the station's downtime (because of the local survey) can be reduced. To observe the radio telescope while the telescope is operating, the surveying strategy has to be modified and additional parameters such as the telescope orientation-angle are necessary.

The first set of approximate values for the main least-squares model can be derived by a damped Gauß–Newton method called the Levenberg–Marquardt algorithm. This hybrid method provides reliable (robust) values.

2. Definitions

2.1. *Coordinate systems*

The established mathematical model includes a transformation between two different mathematical (right-handed) Cartesian coordinate systems. The first is the standard observation system of the terrestrial survey instrument, and the second the telescope system. The observation system is normally (a part of) the local site network at the station. As a rule, this one is realised by stable surveying pillars with forced-centring facilities. The telescope system is defined by the following:

- origin of the coordinate system is the reference point,
- the x-axis is parallel to the elevation-axis,
- the z-axis corresponds to the azimuth-axis of the telescope, and
- the y-axis is normal to the x- and z-axis.

This one rotates around the z-axis relative to the fixed observation system of the survey instrument by the azimuth-angle.

2.2. *Irregularities*

The transformation between these two coordinate systems defined in Section 2.1 can not be described by seven parameters because:

1. The elevation-axis and the azimuth-axis do not intersect; there is an eccentricity between these axes.
2. The elevation-axis and the azimuth-axis are not orthogonal; therefore, there is a small correction angle.
3. The azimuth-axis and the z-axis of the observation coordinate system are not parallel to each other and differ by a small inclination angle.

See Figure 1. The positions of the observation-targets on the side of the telescope are arbitrary. The depen-

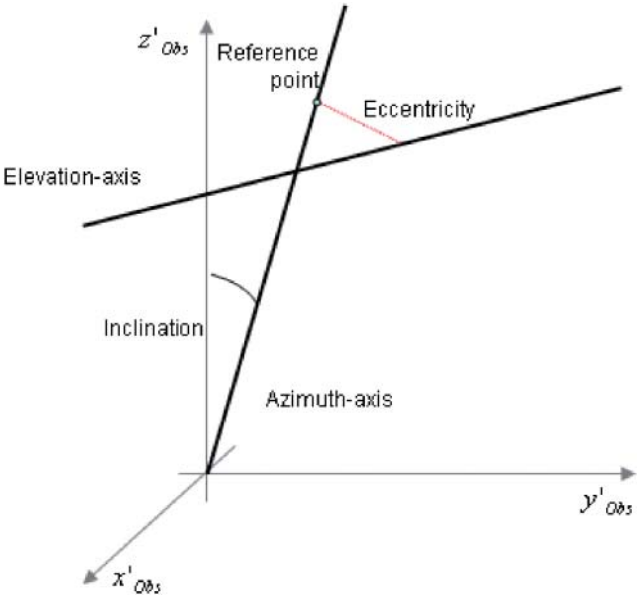

Figure 1: Irregularities: eccentricity and inclination.

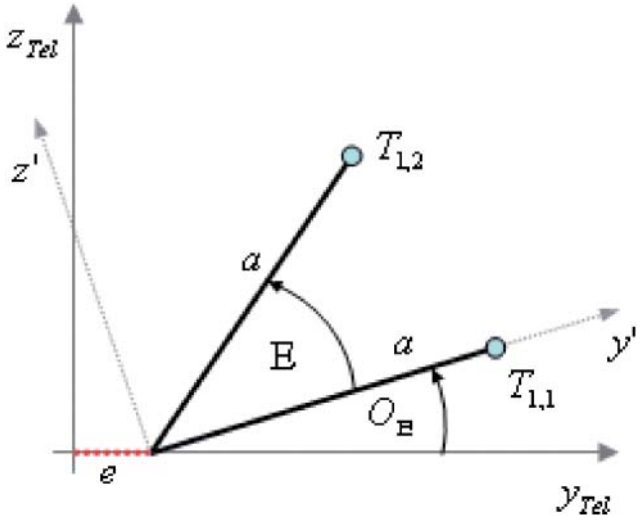

Figure 2: Target position after elevation rotation with correction angle.

dence between the targets and the orientation-angles is shown in Figure 2 and 3 and are dependent only on the direction of the rotation and the magnitude of the angle between two telescope orientations. The position of the target is arbitrary and therefore unknown. Hence the direction of reference (in elevation and azimuth) for the specific target is unknown, too. In order to use the azimuth- and elevation-angle of the telescope to transform a point between the two coordinate systems, there is one azimuth and a specific elevation orientation angle for every target needed.

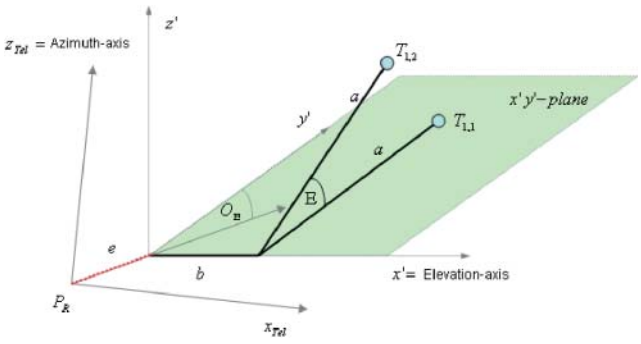

Figure 3: Telescope system and unknown parameters.

3. Local terrestrial survey

The local site network at the Wettzell (Germany) station consists of approximately 50 survey monuments. The larger part of the network is realised by concrete survey pillars with forced-centring facilities. Only a small part of this network around the radio telescope is used for the reference point determination. The observation configurations prohibit a redundant survey of the target on the telescope side to verify the new mathematical model because every telescope position is unique. Thus every target position can be observed only once (in one face) by the survey instrument. For this survey the Leica tacheometer TCRA1201 was employed. The distance accuracy is specified by the manufacturer as $\sigma_{\mathrm{Dist}} = 2\ \mathrm{mm} + 2\ \mathrm{ppm}$ and the accuracy of both, the direction and the vertical-angle, as $\sigma_{Hz} = \sigma_V = 0.3$ mgon for one measurement in two faces. These a priori accuracies were adjusted during the network adjustment. In the final analysis these accuracies were set to $\sigma_{\mathrm{Dist}} = 0.3\ \mathrm{mm} + 2\ \mathrm{ppm}$ and $\sigma_{Hz} = \sigma_V = \sqrt{(0.5\ \mathrm{mgon})^2 + \left(\frac{\sigma_p}{s} \cdot \frac{200}{\pi}\right)^2}$.

Thus the obtained distance precision was much better than the manufacturer's claim. Laboratory investigations at the Geodetic Institute of the University of Karlsruhe confirm this value. However, the precisions of direction and vertical-angle measurements are a little poorer than claimed by the manufacturer depending on the measurement distance s due to additional pointing-error of $\sigma_p = 0.5$ mm.

The local survey was carried out in two observation campaigns. Each consisted of twelve different stations stepped by 30° around the telescope, with two targets on each telescope side. The position of the tacheometer at each station was determined by the free-stationing technique into the local site network. For evaluation purposes, an equal distribution of target positions should be achieved. Therefore, the telescope was moved to predefined positions. The stepping angle around the elevation-axis was $\Delta\mathrm{E} = 10°$ and around the azimuth-axis it was $\Delta\mathrm{A} = 30°$. To minimise environmental influences, which distort the

measurement, the target observation of the telescope from every station was split into two parts with separate free-stationing. In total there were two campaigns, 48 tacheometer stations and 8 target positions, with 960 different positions of the VLBI radio telescope.

A consideration of the correlations between the observed 3D points at the radio telescope is necessary for a reliable determination of the coordinates of the reference point and their accuracy. Thus strict error propagation is required. This can be achieved by a 3D network adjustment to obtain the complete variance-covariance-matrix, which contains the accuracy of a single observation and its covariance with other observations. After the 3D network adjustment the calculated mean point accuracy of an observed point at the telescope, which was measured only once and in one face, was $\hat{\sigma} = 0.5$ mm in each coordinate component taking into account the accuracy of the (fixed) points from the local site network. In addition to the terrestrial survey of the targets on the telescope, the telescope orientation angles A (Alpha) and E (Epsilon) were determined. Hence one complete observation set includes the 3D position of the specific target $T_{i,\mathrm{epo}_{T_i}}$ and the telescope orientation angles $\mathrm{A}_{i,\mathrm{epo}_{T_i}}$ and $\mathrm{E}_{i,\mathrm{epo}_{T_i}}$, where i is the number of the specific target and epo_{T_i} the associated observation epoch.

4. Reference point determination

4.1. *Brief description of the new mathematical model*

The new mathematical model includes the transformation between the two defined coordinate systems, taking into account the irregularities mentioned in Section 2.2.

This transformation can be described by the equation

$$\boldsymbol{P}_{\mathrm{Obs}} = \boldsymbol{P}_R + \boldsymbol{R}_x(\beta) \cdot \boldsymbol{R}_y(\alpha) \cdot \boldsymbol{R}_z(\mathrm{A} + O_{\mathrm{A}}) \cdot \boldsymbol{R}_y(\gamma) \cdot \mathrm{Ecc} + \boldsymbol{R}_x(\mathrm{E} + O_{\mathrm{E}}) \cdot \boldsymbol{P}_{\mathrm{Tel}} \quad (1)$$

where $\boldsymbol{R}$ denotes a rotation matrix for a rotation with a specific angle around the axis indicated in the subscript; $\boldsymbol{P}$ is a 3D point which is transformed from the telescope coordinate system $\boldsymbol{P}_{\mathrm{Tel}}$ into the observation coordinate system $\boldsymbol{P}_{\mathrm{Obs}}$; the azimuth-angle and the elevation-angle of the telescope are denoted by A and E respectively, with the associated orientation angles O_{A} and O_{E}; and the distance between the azimuth-axis and the elevation-axis is the eccentricity e, with $\mathrm{Ecc} = [0, e, 0]^T$. The angle γ is necessary to compensate the non-orthogonality between these axes; the angles α and β are essential to correct for the inclination and to preserve the parallelism condition between the z-axes z_{Obs} (of the observation system) and z_{Tel} (of the telescope system); and the translation vector $\boldsymbol{P}_R$, which points to the reference point itself. A detailed derivation and analysis of this algorithm is given in Lösler and Hennes (2008).

With the three transformation equations – one for each coordinate-component – the reference point can be derived by a least-squares adjustment. It is obvious that each transformation equation contains more than one observation. Because of this, an implicit model known as the Gauß–Helmert model is used to solve the non-linear least-squares problem.

The vector $\hat{\boldsymbol{L}}$ contains the estimated values from the ith target T_i of the real observation $\boldsymbol{L}$. This observation vector can be written as

$$\hat{\boldsymbol{L}}_i = \boldsymbol{L}_i + \mathbf{v}_i = [X_{i,1}, Y_{i,1}, Z_{i,1}, \mathrm{A}_{i,1}, \mathrm{E}_{i,1}, \ldots, X_{i,\mathrm{epo}_{T_i}}, Y_{i,\mathrm{epo}_{T_i}}, Z_{i,\mathrm{epo}_{T_i}}, \mathrm{A}_{i,\mathrm{epo}_{Ti}}, \mathrm{E}_{i,\mathrm{epo}_{T_i}}]^T + \mathbf{v}_i \quad (2)$$

where the vector $[X_{i,\mathrm{epo}_{T_i}}, Y_{i,\mathrm{epo}_{T_i}}, Z_{i,\mathrm{epo}_{T_i}}]^T$ contains the 3D coordinates of several telescope targets $T_{i,\mathrm{epo}_{T_i}}$ and $\mathrm{A}_{i,\mathrm{epo}_{T_i}}$ and $\mathrm{E}_{i,\mathrm{epo}_{T_i}}$ are the telescope orientation angles at the associated observation epoch epo_{T_i}. The vector of unknown parameters $\hat{\boldsymbol{X}}$ consists of eight fixed parameters $\hat{\boldsymbol{X}}_{\mathrm{const}}$ and the target-dependent parameters $\hat{\boldsymbol{X}}_{\mathrm{target}}$.

$$\hat{\boldsymbol{X}}_{\mathrm{const}} = [X_{P_R}, Y_{P_R}, Z_{P_R}, e, \alpha, \beta, \gamma, O_{\mathrm{A}}]^T \quad (3)$$

with

- 3D coordinates $[X_{P_R}, Y_{P_R}, Z_{P_R}]^T$ of the reference point $\boldsymbol{P}_R$,
- eccentricity e between the telescope axes,
- small angles α and β to correct for the inclination,
- angle γ to correct for the non-orthogonality between the axes, and
- azimuth orientation correction O_{A}.

$$\hat{\boldsymbol{X}}_{\mathrm{target}} = [a_{T_i}, b_{T_i}, O_{E_{T_i}}]^T. \quad (4)$$

The target-dependent parameters in the vector $\hat{\boldsymbol{X}}_{\mathrm{target}}$ increase by three for every additional target T. This vector contains:

- distance values a and b along the axes, where b is the distance along the x-axis and a is the shortest distance between the position of the specific target T_i and the x-axis of the telescope coordinate system, and
- the elevation correction angle O_{E}.

It follows from above that the degrees of freedom f is

$$f = n - u = 3 \cdot \sum_{\mathrm{epo}=1}^{\mathrm{epo}_{\max}} T_{i,\mathrm{epo}} - (8 + 3 \cdot t) \quad (5)$$

where n is the number of functional equations, u is the number of unknowns and t is the number of targets.

The first step to solve the system of equations $F(\hat{\boldsymbol{L}}, \hat{\boldsymbol{X}})$ is to linearise them by a first-order Taylor

expansion:

$$F(\hat{\boldsymbol{L}},\hat{\boldsymbol{X}}) = F(\boldsymbol{L}+\boldsymbol{v},\boldsymbol{X}^0+\boldsymbol{x}) = \underbrace{F(\boldsymbol{L},\boldsymbol{X}^0)}_{\boldsymbol{w}} + \underbrace{\frac{\partial F(\boldsymbol{L},\boldsymbol{X}^0)}{\partial \boldsymbol{L}}}_{\boldsymbol{B}} \cdot \underbrace{(\hat{\boldsymbol{L}}-\boldsymbol{L})}_{\boldsymbol{v}} + \underbrace{\frac{\partial F(\boldsymbol{L},\boldsymbol{X}^0)}{\partial \boldsymbol{X}^0}}_{\boldsymbol{A}} \cdot \underbrace{(\hat{\boldsymbol{X}}-\boldsymbol{X}^0)}_{\boldsymbol{x}} = 0. \quad (6)$$

The Gauß–Helmert model, which contains the stochastic model and the mathematical model, minimises the function (e.g. Niemeier 2002):

$$\Omega = \boldsymbol{v}^T \cdot \boldsymbol{Q}_{LL}^{-1} \cdot \boldsymbol{v} + 2\boldsymbol{k}^T \cdot (\boldsymbol{B}\boldsymbol{v} + \boldsymbol{A}\boldsymbol{x} + \boldsymbol{w}) \rightarrow \min \quad (7)$$

with the normal equation

$$\begin{bmatrix} \boldsymbol{B}\cdot\boldsymbol{Q}_{LL}\cdot\boldsymbol{B}^T & \boldsymbol{A} \\ \boldsymbol{A}^T & \boldsymbol{0} \end{bmatrix}^{-1} \cdot \begin{bmatrix} -\boldsymbol{w} \\ \boldsymbol{0} \end{bmatrix} = \begin{bmatrix} \boldsymbol{k} \\ \boldsymbol{x} \end{bmatrix} \quad (8)$$

where the Jacobi matrix, which contains the partial derivatives with respect to the parameters $\boldsymbol{X}$, is denoted by $\boldsymbol{A}$. The design matrix of conditions $\boldsymbol{B}$ includes the partial derivatives with respect to the observations $\boldsymbol{L}$. The vector of misclosures is $\boldsymbol{w}$ and $\boldsymbol{Q}_{LL}$ is the cofactor-matrix of the observations $\boldsymbol{L}$. The vector of increments is given by $\boldsymbol{x}$ and the vector $\boldsymbol{k}$ consists of the Laplace multipliers.

The unknown parameters are estimated iteratively. The number of iterations depends on the quality of the approximate values $\boldsymbol{X}^0$.

$$\hat{\boldsymbol{X}} = \boldsymbol{X}^0 + \boldsymbol{x}. \quad (9)$$

Therefore the Levenberg–Marquardt algorithm (Levenberg 1944, Marquardt 1963) is used to obtain a first reliable solution. This is a hybrid algorithm between the method of steepest descent and the Gauß–Newton method, and reliably solves non-linear least-squares problems. Marquardt (1963) describes this method of damped least-squares by the equation

$$(\boldsymbol{A}^T\boldsymbol{A} + \mu\boldsymbol{I})\boldsymbol{x} = -\boldsymbol{A}^T\boldsymbol{w}. \quad (10)$$

Note the added damping parameter μ ($\mu \geq 0$), strictly speaking the product of the scalar μ with the identity matrix $\boldsymbol{I}$ influences the direction and size of the specific step. The algorithm switches to the Gauß–Newton method for a very small value of the damping parameter μ:

$$\boldsymbol{A}^T\boldsymbol{A} + \mu\boldsymbol{I} \cong \boldsymbol{A}^T\boldsymbol{A} \quad (11)$$

and therefore

$$\boldsymbol{x} \cong -(\boldsymbol{A}^T\boldsymbol{A})^{-1}\boldsymbol{A}^T\boldsymbol{w}. \quad (12)$$

On the other hand, the algorithm becomes the method of steepest descent for a large value of μ, if the current solution is far from the correct one. This means that the matrix of normal equations has a dominant diagonal. The method is slow but guarantees convergence:

$$\boldsymbol{x} \cong -\frac{1}{\mu}\boldsymbol{A}^T\boldsymbol{w}. \quad (13)$$

The damping parameter μ has to be adjusted at each iteration step depending on the error reduction:

$$\Omega_{k+1} < \Omega_k \quad (14)$$

where Ω is the sum of squared errors at the kth iteration.

If the current step fails to reduce the errors, the damping parameter has to be increased, otherwise μ will be reduced. Because of this the Levenberg–Marquardt algorithm is adaptive (Lourakis 2005) and more robust than the Gauß–Newton method. Further information is available in Lourakis (2005) and Madsen et al. (2004).

4.2. *Reference point of the Wettzell 20 m radio telescope*

The aforementioned mathematical model was used to estimate the IVS reference point of the VLBI radio telescope at Wettzell (Germany). The full covariance matrix from the 3D network adjustment was taken into account. The telescope orientation angles were assumed to be uncorrelated and their standard deviations set to $\sigma_{\mathrm{A}} = \sigma_{\mathrm{E}} = 0.0005^\circ$. The complete covariance-matrix of the observation $\boldsymbol{C}_{LL}$ was

$$\boldsymbol{C}_{LL} = \begin{bmatrix} \sigma_X^2 & \sigma_{XY} & \sigma_{XZ} & 0 & 0 & \cdots \\ \sigma_{YX} & \sigma_Y^2 & \sigma_{YZ} & 0 & 0 & \cdots \\ \sigma_{ZX} & \sigma_{ZY} & \sigma_Z^2 & 0 & 0 & \cdots \\ 0 & 0 & 0 & \sigma_{\mathrm{A}}^2 & 0 & \cdots \\ 0 & 0 & 0 & 0 & \sigma_{\mathrm{E}}^2 & \cdots \\ \vdots & \vdots & \vdots & \vdots & \vdots & \ddots \end{bmatrix}. \quad (15)$$

As each telescope point was only observed once, and thus without redundancy, any observation outliers could not be identified using a statistical test during the network adjustment. However, the dependence between the different observation types at the same measurement epoch can be used to check the precision of the observations in the new model later. Two m-dimensional statistical tests T_{prio} and T_{post} were implemented to detect outliers. If the null hypothesis H_0 was rejected, the tested observation was deleted. The difference between these tests is that T_{prio} uses the a priori values of σ_0^2 and T_{post} based on the a posteriori variance $\hat{\sigma}_0^2$ (Jäger et al. 2005).

$$T_{\mathrm{prio}}(\hat{\boldsymbol{V}}_i) = \frac{\hat{\boldsymbol{V}}_i^T \cdot \boldsymbol{Q}_{\hat{V}\hat{V}_i}^{-1} \cdot \hat{\boldsymbol{V}}_i}{m \cdot \sigma_0^2} \sim F_{1-\alpha,m,\infty}|H_0 \quad (16)$$

and

$$T_{\mathrm{post}}(\hat{\boldsymbol{V}}_i) = \frac{\hat{\boldsymbol{V}}_i^T \cdot \boldsymbol{Q}_{\hat{V}\hat{V}_i}^{-1} \cdot \hat{\boldsymbol{V}}_i}{m \cdot \sigma_0'^2} \sim F_{1-\alpha,m,f-m}|H_0 \quad (17)$$

whereas $\hat{\boldsymbol{V}}_i$ is the estimated gross error with its associated cofactor-matrix $\boldsymbol{Q}_{\hat{V}\hat{V}_i}$.

$$\hat{\boldsymbol{V}}_i = -\boldsymbol{Q}_{\hat{V}\hat{V}_i} \cdot [\boldsymbol{P} \cdot \boldsymbol{v}]_i, \tag{18}$$

$$\boldsymbol{Q}_{\hat{V}\hat{V}_i} = [\boldsymbol{P} \cdot \boldsymbol{Q}_{vv} \cdot \boldsymbol{P}]^{-1}_{i,i} \quad \text{and} \tag{19}$$

$$\sigma_0'^2 = \frac{\boldsymbol{v}^T \cdot \boldsymbol{P} \cdot \boldsymbol{v} + [\boldsymbol{P} \cdot \boldsymbol{v}]_i^T \cdot \hat{\boldsymbol{V}}_i}{f - m}. \tag{20}$$

$\boldsymbol{Q}_{vv}$ is the covariance matrix of the residuals $\boldsymbol{v}$, f the degrees of freedom, and $\boldsymbol{P}$ is the inverse cofactor-matrix of the observations $\boldsymbol{P} = \boldsymbol{Q}_{LL}^{-1} = \sigma_0^2 \cdot \boldsymbol{C}_{LL}^{-1}$.

With $m = 1$ only a one-dimensional observation can be tested. Applied to the estimation model this means the telescope orientation angles A and E. The quartile K is taken from the Fisher distribution with a probability value $\alpha = 0.1\%$. If $T \geq K$, the precision of the checked observation has been assumed wrongly. Depending on the value of T the 3D point and the accompanying orientation angles were removed, and the estimation process was repeated until the data set was error free. Altogether, thirteen of the 960 observation pairs were detected and deleted from the adjustment. The degrees of freedom were

$$f = n - u = 2841 - 32 = 2809. \tag{21}$$

The first approximate values of the coordinates of the reference point P_R, which were calculated using the Levenberg–Marquardt algorithm, are given in Table 1.

With these values – the other 29 unknown parameters are not shown – the estimation with the Gauß–Helmert model commenced. The threshold value to halt the iterative computation process was set to

$$\max(|\boldsymbol{x}_i|) \leq 1.0E - 10 \tag{22}$$

where $\boldsymbol{x}$ is the vector of increments of the unknown parameters $\boldsymbol{X}$.

The IVS reference point estimation using the Gauß–Helmert model was iterated three times. The final solution for the reference point coordinates and their accuracy is given in Table 2.

The estimated eccentricity offset e between the azimuth-axis and the elevation-axis, which is important in the analysis of VLBI data, was only $e = -0.08$ mm $\pm$ 0.04 mm and therefore not significant.

Of interest are the estimated variance-components for each observation group g (Table 3). These show the influence of the observations on the outcome and enable an evaluation of the apriori accuracy of each observation. The a priori variance-coefficient σ_0^2 was set to $\sigma_0^2 = 0.001$.

The redundancy of the point group is nearly of the same magnitude as the total redundancy, see equation (21). This means that each coordinate-component has a redundancy of almost $r_i \approx 1.0$. The observation is extremely well controlled, but on the other hand the influence c of the ith observation on the estimated unknown parameters is very small because

$$c_i = 1 - r_i. \tag{23}$$

Furthermore, the quotient between the a posteriori and the a priori variance-coefficient of each observation group is nearly 1.0. This means that the mathematical model and the stochastic model are balanced.

Table 1: Approximate values of the reference point in metres.

$X_{P_R}^0$	$Y_{P_R}^0$	$Z_{P_R}^0$
269.71712	187.69012	622.46483

Table 2: Estimated IVS reference point and its accuracy in metres.

	X_{P_R}	Y_{P_R}	Z_{P_R}
Coordinates	269.71715	187.69011	622.46482
Standard deviation	0.00017	0.00016	0.00016

Table 3: Variance-component estimation.

Observation group g	Redundancy r_g	Variance-coefficient $\hat{\sigma}_g^2$
3D-points	2806.03	0.0008
Azimuth-angles	2.40	0.0006
Elevation-angles	0.57	0.0008

4.3. *Result verification*

To verify the estimated reference point coordinates, an independent approximate calculation without strict error propagation can be used. Due to the observation strategy it is possible to estimate the reference point by 3D circle-fitting (Figure 4). This procedure is well documented, e.g. in Eschelbach and Haas (2003). Three additional geometric conditions were considered because two targets per side were observed:

1. Identical targets, which rotate around the same axis, will generate equal radii.
2. The normal vectors of the circular planes will be equal for each rotation for a particular azimuth orientation; these circular planes are parallel to each other.
3. The distance between the parallel circular planes will be constant for each orientation.

All points were included in a least-squares adjustment. The comparison between the estimated results is summarised in Table 4 and shows a very good agreement. The estimated accuracy of the reference point from the verification model is $\hat{\sigma} = 0.2$ mm in each coordinate-component. The differences between the reference points, calculated from the different methods, are very small and in the range of the esti-

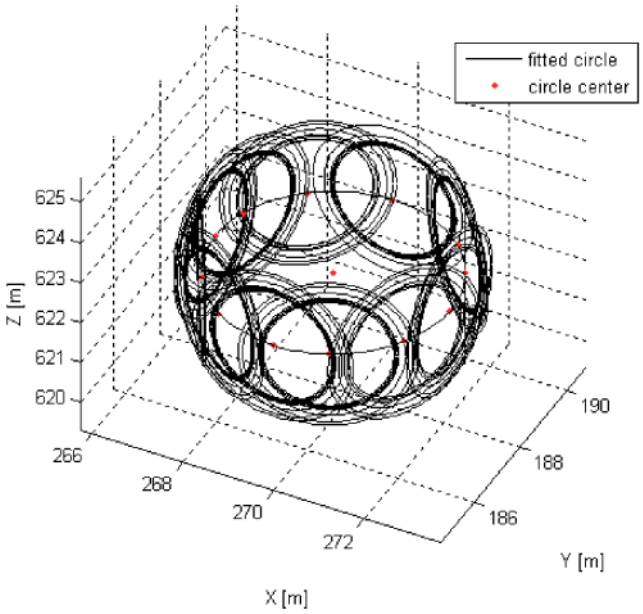

Figure 4: Reference point determination (96 elevation circles and one azimuth circle).

Table 4: Model comparison in metres.

Reference point	New model	Verification	Difference
X_{P_R}	269.71715	269.71720	0.00005
Y_{P_R}	187.69011	187.69008	−0.00003
Z_{P_R}	622.46482	622.46502	0.00020

mated accuracy (1σ). Dawson et al. (2006) has shown that the chosen additional restrictions influence the result of the circle-fitting method more significantly than the differences given in Table 4.

5. Conclusion

To verify a new estimation procedure a reference point determination was carried out at the 20 m VLBI radio telescope at Wettzell (Germany). The IVS reference point was determined using the new mathematical model described in this paper. The achieved accuracy (1σ) of this estimated reference point is $\hat{\sigma} = 0.2$ mm in each coordinate-component and fulfils the demand of the agenda VLBI2010 (Niell et al. 2004). On this account, the described estimation process can be used for permanently monitoring the local ties between the reference points of different space geodetic techniques. Furthermore, the verification with an independent procedure produced a very good agreement.

Acknowledgements

The author is indebted to Dr. Martin Nitschke for discussions during the development on the mathematical model and to the Fundamentalstation Wettzell (Germany), especially to Gerhard Kronschnabl, for support during the fieldwork on the VLBI radio telescope. This research has been supported by Deutsche Forschungsgemeinschaft (DFG), HE5213/2-1.

References

Dawson, J., Sarti, P., Johnston, G., and Vittuari, L., Indirect approach to invariant point determination for SLR and VLBI systems: an assessment, Journal of Geodesy 81 (2006), 433–441.

Eschelbach, C. and Haas, R., The IVS-Reference Point at Onsala – High End Solution for a real 3D-Determination, in: Schwegmann, W. and Thorandt, V. (eds.), Proceedings of the 16th Working Meeting on European VLBI for Geodesy and Astronomy, Germany, Leipzig/Frankfurt a. M., Bundesamt für Kartographie und Geodäsie, May 9–10, 2003, 109–118, 2003.

Jäger, R. R., Müller, T., and Saler, H., Klassische und robuste Ausgleichungsverfahren. Ein Leitfaden für Ausbildung und Praxis von Geodäten und Geoinformatikern, Herbert Wichmann Verlag, Heidelberg, 2005.

Levenberg, K., A Method for the Solution of Certain Problems in Least Squares, Quarterly of Applied Mathematics 2 (1944), 164–168.

Lösler, M. and Hennes, M., An innovative mathematical solution for a time-efficient IVS reference point determination, Proceedings of the FIG2008 – Measuring the changes, Portugal, Lisbon, May 12–15, 2008.

Lourakis, M. I. A., A Brief Description of the Levenberg-Marquardt Algorithm Implemened by levmar. Institute of Computer Science Foundation for Research and Technology – Hellas (FORTH), 2005, available at: http://www.ics.forth.gr/~lourakis/levmar/levmar.pdf (accessed Aug 8, 2008).

Madsen, K., Nielsen, H. B., and Tingleff, O., Methods for non-linear Least Square Problems, Technical University of Denmark, 2nd edition, 2004, available at: http://www2.imm.dtu.dk/pubdb/views/edoc_download.php/3215/pdf/imm3215.pdf (accessed Aug 8, 2008).

Marquardt, D. W., An Algorithm for Least-Squares Estimation of Nonlinear Parameters, Society for Industrial and Applied Mathematics 11 (1963), 431–441.

Niell, A., Whitney, A., Petrachenko, B., Schlüter, W., Vandenberg, N., Hase, H., Koyama, Y., Ma, C., Schuh, H., and Tuccari, G., IVS Memorandum – VLBI2010: Current and Future Requirements for Geodetic VLBI Systems. IVS Memorandum, 2004, available at: ftp://ivscc.gsfc.nasa.gov/pub/memos/ivs-2006-008v01.pdf (accessed Aug 8, 2008).

Niemeier, W., Ausgleichungsrechnung, Walter de Gruyter, Berlin, 2002.

Received: Jun 3, 2008 Accepted: Jul 29, 2008

Author information
Michael Lösler
Geodetic Institute
University of Karlsruhe (TH)
Englerstr. 7
76128 Karlsruhe, Germany
E-mail: michael.loesler@gik.uni-karlsruhe.de